Comparative Assessment of Two CFD Solvers For The Aerodynamic Performance Prediction of Helicopter Components

Enrico Gasparella
PostgraduateResearcher
Dept. of Mechanical Engineering,
University of Padova
Via Venezia, 1 - 35131 Padova - Italy
enrico.gasparella@gmail.com

Rita Ponza
Senior Researcher
HIT09 S.r.l.
Aerodynamics Dept.
r.ponza@hit09.com

Ernesto Benini
Professor
Dept. of Mechanical Engineering,
University of Padova
Via Venezia, 1 - 35131 Padova - Italy
ernesto.benini@unipd.it

ABSTRACT

A comparative assessment of two CFD solvers, namely the open-source solver OpenFOAM® 1.7.x and the commercial ANSYS Fluent® 12, for the prediction of aerodynamic performance of helicopter components is carried out. In particular, the comparison deals with both simple helicopter components having rather poor mesh quality (beanie test case) and more complex analyses of rotating hubs and fuselages with more accurate mesh quality. The obtained results are analyzed and discussed.

INTRODUCTION

The most recent tiltrotor concepts share some advantageous features of the traditional tiltrotors with the tilt-wing aircraft, i.e. the capability of tilting the outboard portions of the wings independently from the proprotos [1],[10],[11]. This means that the new configuration removes the requirement of additional rotor thrust due to the downwash of the rotors on the wings in helicopter mode, reducing the rotor dimension and improving the cruise performance. This translates immediately in the requirement for minimum vehicle drag which is in fact becoming one of the key issues on aeronautics.

The European-funded CODE-Tilt project [1] is aimed at setting up a comprehensive basic "optimal design" procedure with the objective of optimizing some critical components of the new tiltrotor fuselage (e.g. the nose, the wing-fuselage junction and the sponson) in order to improve the overall efficiency of the aircraft. Within the CODE-Tilt research project, a comparative study is being carried out with the purpose of evaluating the use of both an open source CFD code, OpenFOAM®, and a commercial one, ANSYS Fluent, as key-parts of the optimization tool.

Some interesting studies on CFD optimization using OpenFOAM® are presented in [8] and [9] which include some external aerodynamictestsregarding incompressible flows. In the former work, the author presented a fast gradient-based optimization method for automotive flow design using the OpenFOAM® toolbox in its incompressible flow formulation. In the latter, the proposed method relies on GRIA, a middleware for deploying data and job services within a Grid environment. The CFD code OpenFOAM® was customized and deployed through GRIA as a Grid service to perform large number of fluid design evaluations in a remote HPC cluster again using an incompressible flow formulation.

The main objective of the present work is to understand whether or not OpenFOAM® is a reliable and efficient tool for drag and lift calculation of helicopter components.

From a previous comparative assessment of pure CFD capabilities [2],[4] (without any optimization target), a general compressible analysis showed that the basic OpenFOAM® configuration had difficulties in solving transonic flows over standard NACA and RAE airfoils in a competitive way (in comparison with ANSYS Fluent® steady state compressible solver), highlighting the lack of an effective and fast density-based solver. Some customized routines have been successfully developed in-house [3],[4]aimed at fixing such problems. However, often these new solvers implements a transient model and are not competitive in terms of simulation time (since a transient model is too slow in comparison with a steady state one).

On the other hand, standard OpenFOAM® solvers have given interesting results in analyses of fully subsonic flows, while exhibiting a noticeable inaccuracy in calculating the drag coefficient (in comparison with both experimental and ANSYS Fluent® results), a fact which is probably associated with a difficult assignment of similar ANSYS Fluent® boundary conditions [2].

In this work, a comparative analysis of the two CFD solvers is focused on helicopter components. In particular, analyses of fuselage and helicopter components in forward flight configuration, as well as analyses of the hub main rotor in subsonic and stationary flow, both in forward flight and hovering configurations, are described. To this purpose, the same mesh was processed in order for a coherent comparison between the two codes to be carried out.

HELICOPTER FUSELAGE

This test case concerns steady state simulations of a full scale helicopter fuselage at subsonic flow regime, specifically, a forward flight condition with a forward speed equal to 120 kts at ISA Sea Level conditions and at null angle of attack was analyzed (Table 1). A global view of the domain is illustrated in Figure1.

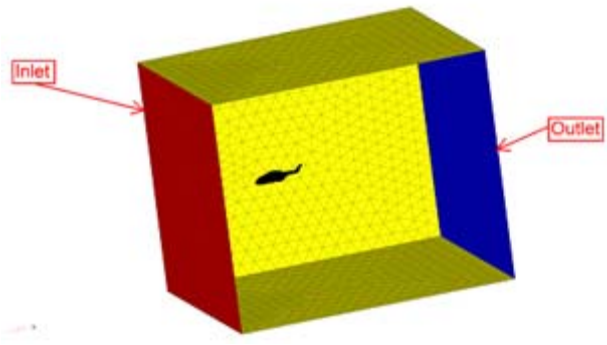

Figure 1. Helicopter computational domain

Operating conditions	
Static pressure	101,325 Pa
Static temperature	288.15 K
Speed	120 kts
Mach number	0.18
fuselage incidence angle	0 deg

Table 1. Helicopter fuselage operating conditions

	Inlet	**Outlet**
U	pressureInletVelocity	pressureInletOutletVelocity
p	totalPressure	fixedValue
T	totalTemperature	inletOutletTotalTemperature
k	fixedValue	inletOutlet
ω	fixedValue	inletOutlet

Table 2. OpenFOAM® boundary condition for helicopter fuselage (inlet and outlet BC)

A mesh was generatedusingANSYSTgrid® from a surface mesh created with CATIA® and it was kept unchanged for both the CFD codes. This generic isolated fuselage geometry was developed in house at UNIPD (University of Padova) in order to be representative of a standard medium-heavy class helicopter formed by main fuselage, two engine cowlings, landing gear fairings (sponsons) and a rear ramp.

OpenFOAM® Boundary Condition and Setup

The fuselage analysis was carried out using the *rhoSimpleFoam* standard OpenFOAM® solver (version 1.7.x), a steady-state SIMPLE solver for laminar or turbulent RANS compressible flow. The air was treated as a turbulent, compressible ideal gas, with standard properties [5].The Wilcox's two-equation k-ω model with the Shear-Stress-Transport correction (SST) [7] has been chosen with a Kinetic Energy value k=3.4m^2/s^{2}and a Specific Dissipation Rate value ω=4.2s^{-1}calculated from standard Fluent-like formulas:

$$k=3/2\ (u_{avg}I)^2;\ \omega=\sqrt{k}/(C_\mu)^{0.25}\ l$$

where u_{avg} is the mean flow velocity, I the turbulence intensity, C_μ an empirical constant specified in the turbulence model (approximately 0.09) and l the length scale.

The computational mesh included the inlet and outlet boundaries of the "patch" type, the fuselage surface with patch type "wall" and the wind tunnel lateral wall with patch type "*symmetryPlane*". The variables U, p, T, k and ω were calculated based on the operating conditions and the boundary conditions used at inlet and outlet for each of the above mentioned variables are summarized in Table 2. Regarding the fuselage, a standard set of boundary condition was selected (velocity fixed with 0m/s value at the surface and *zeroGradient*for p and T) and the k-ω SST standard wall functions were activated [5].

The OpenFOAM® wall functions in their compressible version were selected over all the fuselage surface patches. Finally, a *symmetryPlane* condition was assigned over the lateral walls of the virtual wind tunnel surrounding the fuselage.

OpenFOAM® Solution Strategy

The first calculation was run using numerical schemes of the first order type using the *upwind* (First order, bounded) scheme; then, once the solution was converged, it was used as a starting point for first/second order type numerical schemes. The first/second order schemes selected were *Gauss Linear* (Second Order, Gaussian integration) with cell limited option for gradient, *linearUpwind* schemes (First-Second Order, bounded) with cell limited option for divergence, *linearLimited* for laplacian and a *linear* scheme for interpolation. In the solver setup (fvSolution), a tolerance of 10^{-9} was selected with a 0.1 relative tolerance. The final relaxation factors were 0.3 for p and rho, and 0.7 for the other quantities (i.e. ωand k).

ANSYS Fluent® Boundary Condition and Setup

A pressure-based solver type with absolute velocity formulation and steady approach was used for the helicopter fuselage steady simulations within ANSYS Fluent®. The k–ω SST turbulence model was selected for the simulation of viscous effects. Air was treated as an ideal gas having constant specific heats, which automatically enabled the energy equation resolution. Fluid viscosity was modeled using the pre-defined three-coefficient Sutherland law. The following boundary conditions were prescribed: a total pressure condition was imposed on the wind tunnel inlet, while a static pressure was assigned on the outlet section. Total pressure and total temperature were calculated based on the static pressure, static temperature and speed of the selected operating condition. The fuselage surface was treated as a hydraulically smooth and adiabatic wall, while a symmetry condition was used for the lateral surfaces of the wind tunnel box. As far as the turbulence specification method is concerned, the turbulence kinetic energy k and the specific dissipation rate ω were specified with the same value of OpenFOAM®.

ANSYS Fluent® Solution Strategy

A SIMPLE scheme was adopted as the solution algorithm for the simulations. The selected discretization scheme was the Third Order MUSCL, since a higher order is suggested for improving the solution accuracy, despite the increase in simulation time [6]. The under-relaxation factors were left unchanged to their default values. Moreover, the solution was initialized by assigning the fluid values of the inlet section over the fluid domain except for the velocity vector, which was given a value of (5,0,0) [m/s], and by using an absolute reference frame, in order for the iterative process to start from a reasonable solution and speed up the convergence. The convergence criterion was established when the RMS residuals were less than 10^{-4}.

RESULTS

A comparison between OpenFOAM® CFD simulations and ANSYS Fluent® calculations will be presented in terms of static pressure coefficient distribution over the fuselage, total pressure losses downstream of the fuselage and global aerodynamic coefficients. Contours of pressure coefficient over the fuselage coming from both OpenFOAM® and ANSYS Fluent® simulations are compared in Figure 2.

The results show a very good agreement although some minor discrepancies are evidenced on the helicopter rear ramp, where OpenFOAM® predicts a more pronounced pressure drop over the sharp edge at the beginning of the

ramp and a more rapid pressure rise along the ramp itself towards the empennages, as also confirmed by the 2D longitudinal midsection of pressure coefficient in Figure 3. However, overall correlation in the static pressure coefficient between the two codes is very satisfactory and negligible differences are found, as can be appreciated mainly from the 2D sections of the Cp distribution.

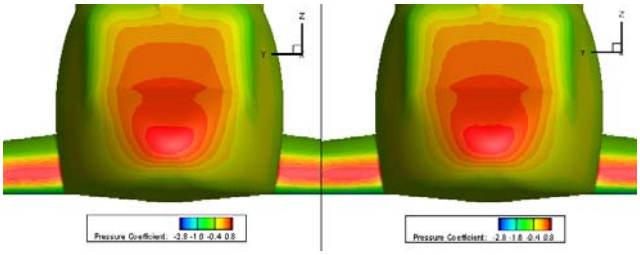

Figure 2. Frontal view of the pressure coefficient contour plot over the fuselage: comparison of OpenFOAM® (on the right) and ANSYS Fluent® (on the left) results.

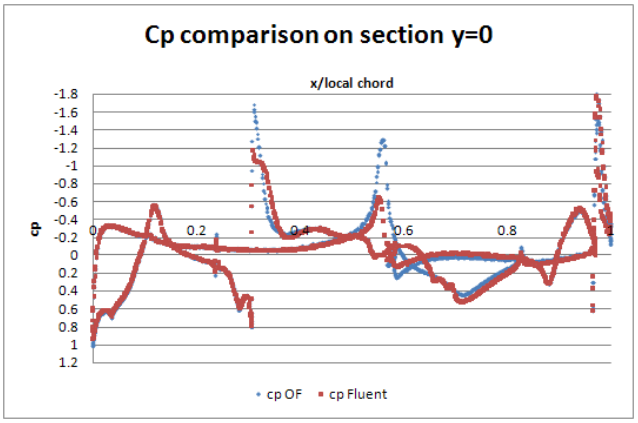

Figure 3. Cp distribution over the fuselage surface over the longitudinal midsection: comparison of OpenFOAM® and ANSYS Fluent® results.

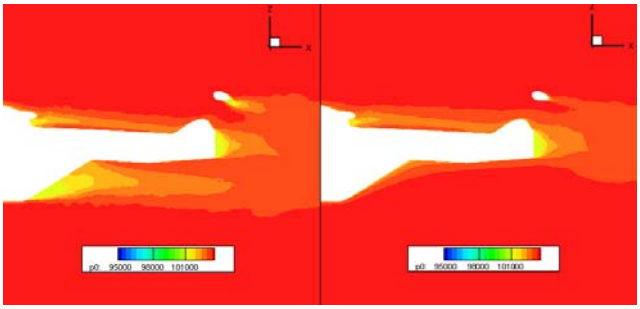

Figure 4. Contours of total pressure over the fluid domain longitudinal midsection: comparison of OpenFOAM® (on the right) and ANSYS Fluent® (on the left) results.

Both ANSYS Fluent® and OpenFOAM® contour plots of the total pressure are provided in the longitudinal midsection of the fluid domain (Figure 4): local dissipative phenomena are found which are related mainly to the presence of separated flow regions close to the rear ramp. However, total pressure losses predicted by ANSYSFluent® are much larger than those calculated by OpenFOAM® in this region.

OpenFOAM® simulations show a flow attached to the fuselage surface but ANSYS Fluent® show a much larger flow recirculation. The reason for this behavior is still unclear. However, it is probablyduethe different implementation of the turbulence models in the two CFD codes; such argument could also explain the differences in the static pressure distribution over the rear portion of the fuselage. On the other hand, pressure losses downstream of the engine upper deck over the top of the fuselage compare very well. As apparent, all OpenFOAM® residuals fall under 10^{-6} and appear slightly more stable than ANSYS Fluent® ones: moreover, ANSYS Fluent® residuals are stabilized over much higher mean values than those achieved with OpenFOAM®, especially as far as the continuity residual is concerned. This could be probably explained with the remarkable flow detachment found in the ANSYS Fluent® simulation over the fuselage rear ramp, which is likely to introduce unsteady phenomena, hence making the steady-state simulation intrinsically unstable. In addition, in Table 3 the computed values of the global aerodynamic coefficients of the fuselage using the two CFD codes are summarized. Concerning the drag coefficient, a very satisfactory agreement is shown between the two codes, with OpenFOAM® drag coefficient being 2.1% lower than the ANSYS Fluent® value: as apparent, the pressure contribution to drag is predominant according to both OpenFOAM® and ANSYS Fluent®, and the former tends to underestimate it by 5%. On the other hand, predictions in the lift coefficient show a large misalignment, being the OpenFOAM® value around 76% lower than the ANSYS Fluent® one.

		ANSYS Fluent®	OpenFOAM®	Δ%
CL	**Total**	**0.004377**	**0.001054**	**-76%**
	pressure	0.004371	0.001049	-76%
	viscous	$5.8 \cdot 10^{-6}$	$5.65 \cdot 10^{-6}$	-2.5%
CD	**Total**	**0.007469**	**0.007309**	**-2.1%**
	pressure	0.006025	0.005718	-5%
	viscous	0.001444	0.001591	10%
CY	**Total**	**0.002598**	**0.003147**	**21.1%**
	pressure	0.002588	0.003144	21.5%
	viscous	$1.02 \cdot 10^{-5}$	$3.3 \cdot 10^{-6}$	-67.8%

Table 3. Aerodynamic force coefficients of the fuselage: comparison of OpenFOAM® and ANSYS Fluent® results.

Operating conditions	
Static pressure	101,325 Pa
Static temperature	293.15 K
Speed	40 m/s
Mach number	0.117
beanie incidence angle	0 deg
rotational speed	31 rad/s

Table 4. Main rotor beanie operating conditions

The reason for this is not clear so far and needs further investigation, especially considering the optimum correlation on the static pressure coefficient distribution over the fuselage illustrated above. As far as the side force coefficient is concerned, a 21% deviation was found, mainly due to the pressure contribution, as OpenFOAM® overpredics it with respect to the ANSYS Fluent® simulations.

MAIN ROTOR BEANIE

This test case is carried out in order to assess OpenFOAM® capabilities on 3D helicopter components configurations concerns both steady state and rotating simulations (using the MRF approach) of the full scale helicopter beanie at subsonic flow regime: specifically, a forward flight condition with a forward speed equal to 40 m/s at null angle of attack was analyzed. 31 rad/s was selected as operational angular speed.

The selected operating conditions for the beanie are reported in Table 4.

STEADY BEANIE IN FORWARD FLIGHT CONDITIONS

First of all, a non-rotating beanie in forward flight conditions was analyzed.
A global view of the computational domain around the beanie is given in Figure 5.
This mesh was created with ANSYSTgrid® from a starting surface mesh created with CATIA®. The mesh was the same for the both CFD codes. Apparently, the dimensions of the virtual wind tunnel are too small for the numerical simulation to be accurate, and the mesh is rather coarse: however, emphasis here is on the numerical model feasibility rather than on its accuracy, as well as on the comparison between the two involved CFD solvers at given mesh characteristics, while a detailed analysis of the simulations' accuracy goes beyond the scope of this work.

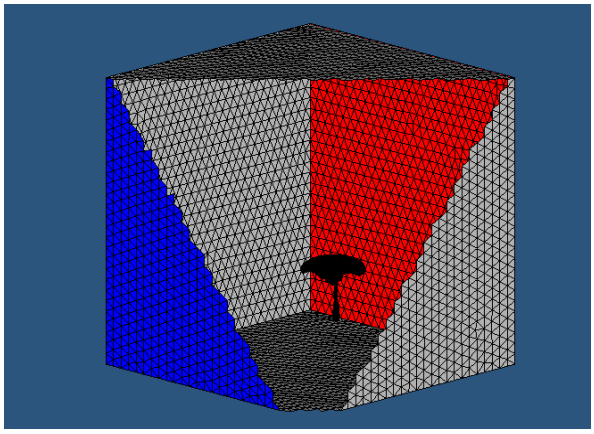

Figure 5. Forward flight beanie computational domain

OpenFOAM® Setup
The beanie analysis was carried out again using the *rhoSimpleFoam* standard OpenFOAM® solver (version 1.7.x). The k-ω SST turbulence model was selected for simulation of viscous effects. As far as the setup of the boundary conditions and solution strategy were the same of the helicopter fuselage setup discussed above, with a Kinetic Energy value $k=1.6m^2/s^2$ and a Specific Dissipation Rate value $\omega=2.9s^{-1}$.

ANSYS Fluent® Setup
A steady pressure-based solver type with absolute velocity formulation was used for the non-rotating beanie steady simulations within ANSYS Fluent®. The convergence criterion was established when the RMS residuals were less than 10^{-4} and the other setup variables were the same of those used in the fuselage test.

RESULTS
The contours of pressure coefficient over the beanie coming from OpenFOAM® and ANSYS Fluent® simulations were compared and an excerpt is reported in Figure 6. As apparent, also in this case correlation of OpenFOAM® results with ANSYS Fluent® is very satisfactory, especially as far as the upper surface of the beanie is concerned.
On the other hand, some discrepancies are found over the lower surface; in particular, OpenFOAM® predicts a smaller mean value of the static pressure over the beanie lower midsection downstream of the supporting system. This seems consistent with the results already found regarding the helicopter fuselage.

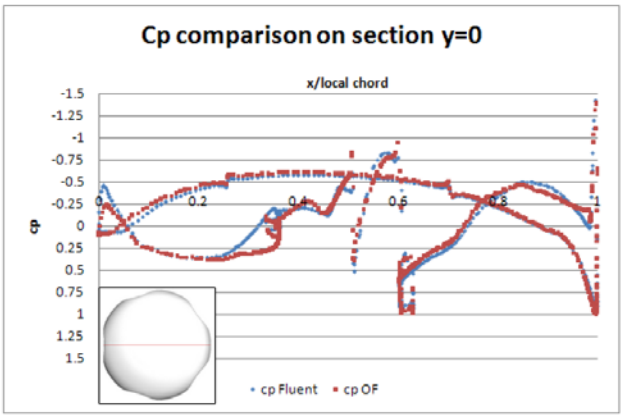

Figure 6. Cp distribution over the beanie surface over the longitudinal midsection: comparison of OpenFOAM® and ANSYS Fluent® results.

Again, this is probably due to a different implementation of the turbulence models and wall functions in the two codes. Furthermore, both ANSYS Fluent® and OpenFOAM® contour plots of the total pressure are provided in the longitudinal midsection of the fluid domain (Figure 7). From this plot, the amount of local dissipative phenomena downstream of the beanie can be appreciated. As can be observed, total pressure losses prediction using the two codes is in excellent agreement. Actually, wake intensity (in terms of vorticity) predicted by ANSYS Fluent® in this region is higher than that simulated using OpenFOAM®, which could justify the above mentioned more pronounced pressure drop predicted by ANSYS Fluent® over this section. Furthermore, a large flow separation is found over the fore portion of the beanie lower surface and downstream of the supporting system, where the lower portion of the beanie wake tends to be absorbed into the pylon wake. The total pressure field predictions downstream of the supporting system are in very good agreement, even though wake losses predicted by ANSYS Fluent® are slightly less intense.

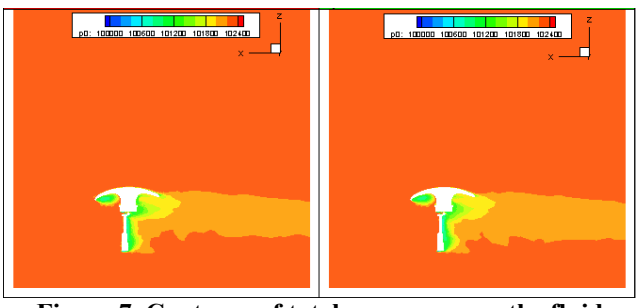

Figure 7. Contours of total pressure over the fluid domain longitudinal midsection: comparison of OpenFOAM® (on the right) and ANSYS Fluent® (on the left) results.

In addition, in Table 3 the computed values of the global aerodynamic coefficients of the non-rotating beanie using the two codes are reported.

As far as the lift coefficient is concerned, a satisfactory agreement is shown between the two codes, the lift coefficient by OpenFOAM® being 16% higher than the ANSYS Fluent® value: these differences may be justified with the above mentioned misalignments in the static pressure distributions over the beanie, especially concerning the lower region, where flow detachment occurs.
On the other hand, correlation on drag coefficient is very good, with a global difference between the two codes of around 7.5%.

		ANSYS Fluent®	OpenFOAM®	Δ%
CL	**Total**	**0.000908**	**0.001055**	**16.2%**
	pressure	0.000909	0.001055	16.1%
	viscous	-9E-07	-4.2E-07	-53%
CD	**Total**	**0.000628**	**0.000674**	**7.5%**
	pressure	0.000597	0.000646	8.1%
	viscous	3.06E-05	2.89E-05	-5.4%

Table 3. Aerodynamic force coefficients of the forward flight beanie: comparison of OpenFOAM® and ANSYS Fluent® results.

ROTATING BEANIE IN FORWARD FLIGHT CONDITIONS

A second beanie simulation using a moving reference frame option was selected which is a steady-state approximation in which individual grid zones move at different rotational and/or translational speeds. The flow in each moving zone is solved using the moving reference frame equations, while in the stationary regions the stationary equations are applied. As already mentioned, the relative motion of a moving zone with respect to adjacent zones is not taken into account in the MRF approach; in other words, the grid remains fixed in the computation. A global view of the computational domain around the rotating beanie is illustrated in Figure 8. Again, the mesh was generated using ANSYSTgrid® from a surface mesh created with CATIA® and it was the same for the both CFD code simulations.

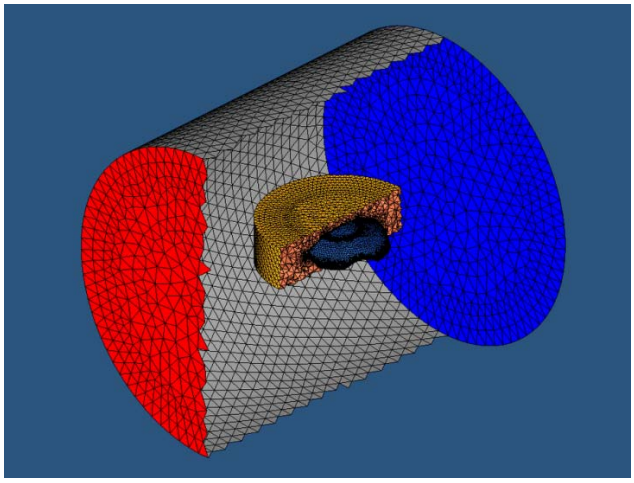

Figure 8. Rotating beanie computational domain

The analyzed geometry is the same as the one used in the previous section; however, for the sake of simplicity, only the beanie was considered here, while both the balance and the supporting system were removed from the geometrical model. In order for the MRF approach to be successfully applied, two distinct zones needed to be defined in the fluid domain. To this purpose, an external cylindrical box was created first to simulate the stationary virtual wind tunnel. Then, the beanie was embedded into an internal cylinder, representing the rotating portion of the domain. Also in this case, the dimensions of the virtual wind tunnel are insufficient to avoid blockage effects and the mesh itself is rather coarse: however, the emphasis here is on the numerical model feasibility, and on the comparison between the two involved CFD solvers at given mesh characteristics, while a detailed analysis of the simulations' accuracy goes beyond the scope of this work.

OpenFOAM® Setup

The beanie analysis was carried out using a steady-state *rhoMRFSimpleFoam* solver. This new solver was implemented by UNIPD [2] and was based on the updated version (OpenFOAM® 1.7 release) of the rhoSimpleFoam solver, able to handle rotating regions with a MRF approach using a steady formulation. Actually, the transient approach of the standardrhoPorousMRFPimpleFoam solver appears unnecessary for steady-state simulations of rotating components which we are interested in. The k-ω SST turbulence model was selected for simulation of viscous effects. Moreover, the rotating cylinder surrounding the beanie (called "fluid-16") was specified to belong to the MRF portion of the domain, hence it was defined within the MRFZones file as a rotating region, with origin located in (0;0;0), rotation axis coincident with the z axis and rotational speed equal to 31 rad/s. Differently from ANSYS Fluent® MRF setup, the interface between the inner, rotating cylinder and the external domain is read as an internal patch within OpenFOAM®, so that no boundary conditions needed to be specified over this surface. To this purpose, it is worth highlighting that, in order for the domain with the stationary and rotating fluid volumes to be successfully imported within OpenFOAM, the duplicate interface surfaces belonging to both the fixed and rotating portions are to be connected and the model needs to feature a single superficial mesh over the interface between the two volumes. The setup of the other boundary conditions and solution strategy were the same of the steady non-rotating beanie. As it is well known, the rotation of the reference frame can give rise to complex disturbances in the flow, hence the residuals may be less stable as the rotational speed increases. In order to overcome this complication and prevent numerical instabilities, the simulation in rotating conditions did not start with the nominal value of rotational speed: the angular velocity was instead slowly increased in some steps until the operating speed was reached. In particular, four incremental steps were carried out with rotational speed equal to 5, 10, 20 and 31 rad/s respectively. Alternatively, the rhoMRFSimpleFoam solver can stand the nominal angular speed since the first iterations, provided that the under-relaxation factors are adequately decreased.

ANSYS Fluent® Setup

A steady pressure-based solver type with absolute velocity formulation was used for the simulations within ANSYS Fluent®. However, MRF analyses required some adjustments in the boundary conditions. In fact, the fluid zone contained in the rotational reference frame had to be changed from steady to moving reference frame entering the required parameters. Furthermore, the wall zone representing the beanie was changed from a stationary wall to a moving wall condition. Since the wall rotates at the

same speed of the rotating frame, the beanie relative angular speed was set to zero, while the parameters concerning the rotational axis (i.e. point and direction) were the same used for the set up of the fluid zone. A SIMPLE scheme was adopted as the solution algorithm for the simulations. The selected discretization scheme was the Third Order MUSCL, since a higher order is suggested for improving the solution accuracy, despite the increase in simulation time. Finally, no intermediate simulations with successive steps of the angular velocity were necessary, since the calculation with the nominal rotational speed was quite stable. The convergence criterion was established when the RMS residuals were less than 10^{-4} and the other setups were the same of non-rotating beanie test.

RESULTS

The contours of pressure coefficient over the beanie coming from OpenFOAM® and ANSYS Fluent® simulations are compared in Figure 9.

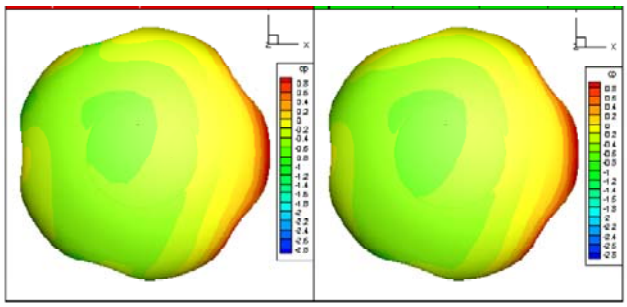

Figure 9. Top view of the pressure coefficient contour plot over the beanie: comparison of OpenFOAM® (on the right) and ANSYS Fluent® (on the left) results.

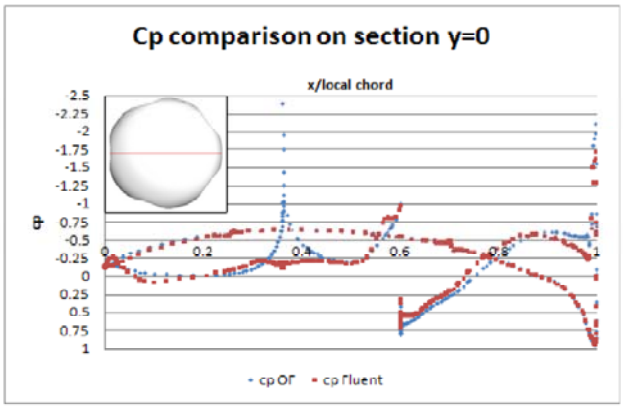

Figure 10. Cp distribution over the beanie surface over the longitudinal midsection: comparison of OpenFOAM® and ANSYS Fluent® results.

A number of longitudinal sections of the beanie were created with the aim of comparing in an accurate way 2D sections of static pressure coefficient distributions calculated using both CFD codes and the results are shown in Figure 10.

As apparent, the correlation of OpenFOAM® results with ANSYSFluent® is very good over the upper surface of the beanie. Specifically, the modifications in the Cp distribution with respect to the stationary simulation are well captured by both the CFD codes: the area of minimum Cp over the beanie upper surface is no longer symmetrical with respect to the flow direction, but it is rather shifted along the negative *y* direction.

The same trend, though symmetrical, is observed at the beanie lower surface. On the other hand, some discrepancies are found over the lower surface; in particular, OpenFOAM® predicts a slightly higher mean value of the static pressure over the beanie lower surface in the $y \geq 0$ region.

Once again this is consistent with the results already found in both the helicopter fuselage and the non-rotating version of the beanie: OpenFOAM® and ANSYS Fluent® are in very good agreement when no flow detachment occurs, while some differences are evidenced over regions of recirculated flow. This is the case for the lower portion of the beanie, where the complexity of the geometry induces a large flow separation, as can be appreciated also in the total pressure contours visualization depicted in Figure 11 (longitudinal midsection of the fluid domain).

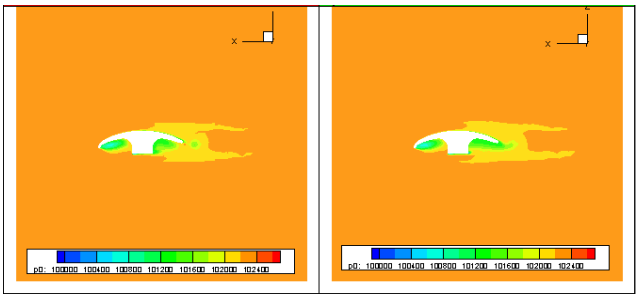

Figure 11. Contours of total pressure over the fluid domain longitudinal midsection: comparison of OpenFOAM® (on the right) and ANSYS Fluent® (on the left) results.

In addition, in Table 4 the computed values of the global aerodynamic coefficients of the rotating beanie using the two codes are reported. Similarly to the non-rotating case, the aerodynamic coefficients of the beanie are in good agreement in theirglobal value.

		ANSYS Fluent®	OpenFOAM®	Δ%
CL	**Total**	**0.00085**	**0.000913**	**7.5%**
	pressure	0.000851	0.000913	7.5%
	viscous	-6.9E-07	-3.5E-07	-50%
CD	**Total**	**0.000598**	**0.000657**	**9.8%**
	pressure	0.000577	0.000631	9.4%
	viscous	2.08E-05	2.5E-05	20%

Table4. Aerodynamic force coefficients of the rotating beanie: comparison of OpenFOAM® and ANSYS Fluent® results.

Concerning the lift coefficient, a satisfactory agreement is shown between the two codes, with OpenFOAM® lift coefficient being 7.5% higher than the ANSYS Fluent® value: once again, these differences may be justified with the above discussed misalignments in the static pressure distributions over the beanie, especially concerning the lower region, where flow detachment occurs. Correlation on drag coefficient is good as well, with a global difference between the two codes of around 10%. Also in this case, the pressure contribution to drag is predominant according to both OpenFOAM® and ANSYS Fluent®, and the former tends to overestimate it by more than 9%. In addition, it is worth noting that both the codes predict a reduction of both the beanie lift and drag with respect to the non-rotating configuration.

MAIN ROTOR HUB

This test case, to be carried out in order to assess OpenFOAM® capabilities on 3D helicopter configurations, concerns both steady state and rotating simulations (using the MRF approach) of the full scale

helicopter hub at subsonic flow regime. Specifically, the steady hub in forward flight at ISA Sea Level conditions with a speed equal to 120 kts and at null angle of attack was simulated. Simulations of the rotating hub with a forward flight speed equal to 120 kts and an angular velocity of 31 rad/s was carried out. Unlike the beanie test case described previously, a single mesh was set up around the hub for both stationary and rotating simulations (this unique mesh was generated using ANSYSTgrid® from a surface mesh created with CATIA® and it was the same for the both CFD codes). To this purpose, the volume surrounding the helicopter hub was split in two portions, and they were handled in a different way for the two kinds of simulations: while both of them were defined as stationary zones for stationary analyses, the hub rotation was simulated using the MRF approach, by assigning to the inner volume a rotational speed and keeping the outer portion of the domain fixed.

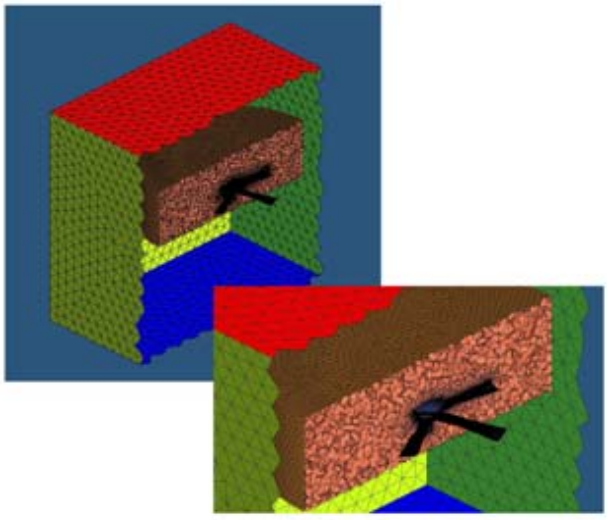

Figure 12. Main rotor hub computational domain

Operating conditions		
Static pressure		101,325 Pa
Static temperature		288.15 K
Forward Speed	**Forward flight**	120 kts
	Hovering	0 kts
Mach number		0.18
Rotational speed		31 rad/s

Table 5. Main rotor HUB operating conditions

STEADY HUB IN FORWARD FLIGHT CONDITIONS

First of all, the non-rotating hub in forward flight conditions was analyzed. A global view of the computational domain around the beanie is illustrated in Figure 12. The computational mesh included the patches inlet and outlet, which were assigned a "patch" type, body (made up of the beanie, shaft and blade stubs), which was defined of the wall type (no slip), and symmetry (wind tunnel lateral walls), which was assigned a symmetryPlane type. The selected operating conditions for the hub are reported in Table 5.

OpenFOAM® Setup

The non-rotating hub analysis was carried out using the rhoSimpleFoam standard OpenFOAM® solver (version 1.7.x), as non-rotating beanie and fuselage analysis. The k-ω SST turbulence model was selected for simulation of viscous effects.As far as the setup of the boundary conditions and solution strategy were the same of the beanie setup in the same analysis condition discussed above, with a Kinetic Energy value $k=3.41 m^2/s^2$ and a Specific Dissipation Rate value $\omega=4.22 s^{-1}$.

ANSYS Fluent® Setup

A steady pressure-based solver type with absolute velocity formulation was used for the non-rotating beanie steady simulations within ANSYS Fluent®. Total temperature, Gauge Total Pressure and Backflow Total Temperature were carried out from initial condition. The convergence criterion was established when the RMS residuals were less than 10^{-4} and the other setup variables were the same of the beanie test.

RESULTS.

The contours of pressure coefficient over the beanie coming from OpenFOAM® and ANSYS Fluent® simulations are compared in Figure 13.

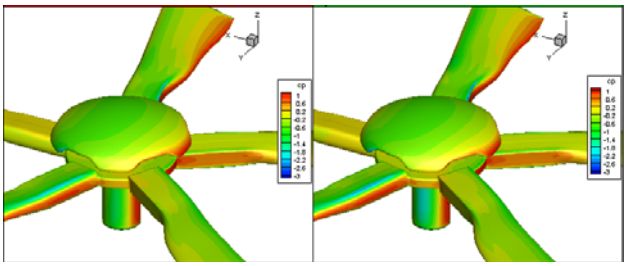

Figure 13. View of the pressure coefficient contour plot over the forward flight main rotor hub: comparison of OpenFOAM® (on the right) and ANSYS Fluent® (on the left) results.

A number of longitudinal sections of the beanie component were created with the aim of comparing in an accurate way 2D sections of static pressure coefficient distributions calculated using both CFD codes: a comparisons is reported in Figure 14, which show the$C_p$distribution of the main rotor hub.From the above mentioned figures it can be argued that the correlation of OpenFOAM® results with ANSYS Fluent® is excellent, both over the beanie upper surface and the blade stubs.

On the other hand, some discrepancies are found over the lower beanie surface: OpenFOAM® predicts a smaller mean value of the static pressure over the beanie lower surface next to the shaft on both sides of the stagnation region. Once again, this is consistent with the results of the previous simulations: as long as no flow detachment occurs, the two codes are in very good agreement, while some discrepancies arise when regions of flow recirculation are evidenced, as is the case for the lower portion of the beanie, where a flow separation is evidenced, as apparent also from contour of total pressure visualization in Figure 15. Concerning the longitudinal midsection, an excellent correlation is found both over the beanie upper surface and the aft portion of the lower surface, while on the lower surface fore portion a mean positive value of the static pressure coefficient is found using OpenFOAM®, while ANSYS Fluent® predicts a slightly negative value (Figure 14).

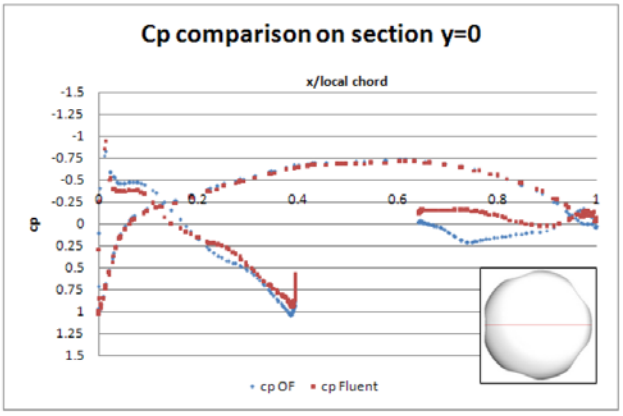

Figure 14. Cp distribution over the main rotor beanie surface over the longitudinal midsection: comparison of OpenFOAM® and ANSYS Fluent® results.

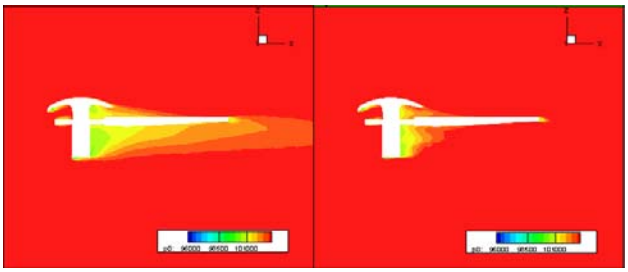

Figure 15. Contours of total pressure over the fluid domain longitudinal midsection: comparison of OpenFOAM® (on the right) and ANSYS Fluent® (on the left) results.

In addition, in Table 6 the computed values of the global aerodynamic coefficients of the rotating beanie using the two codes are reported.

		ANSYS Fluent®	OpenFOAM®	Δ%
CL	**Total**	**0.002117**	**0.001832**	**-13.4%**
	pressure	0.00212	0.001833	-13.5%
	viscous	-2.9E-06	-1.4E-06	-50%
CD	**Total**	**0.002698**	**0.002618**	**-2.97%**
	pressure	0.002458	0.002435	-0.93%
	viscous	0.000241	0.000183	-23.8%

Table 6. Aerodynamic force coefficients of the forward flight main rotor hub: comparison of OpenFOAM® and ANSYS Fluent® results.

Concerning the lift coefficient, a satisfactory agreement is shown between the two codes, where OpenFOAM® lift coefficient is 13% lower than the ANSYS Fluent® value: also in this case, these differences may be justified with the above discussed slight misalignments in the static pressure distributions over the hub, especially concerning the beanie lower region, where flow detachment occurs. On the other hand, correlation on drag coefficient is very good, with a global difference between the two codes of about 3%.

Once again, the pressure contribution to drag is predominant according to both OpenFOAM® and ANSYS Fluent®, and the former tends to slightly underestimate it (-1%) with respect to the ANSYS Fluent® value, while a larger disagreement is shown on the viscous contribution to drag.

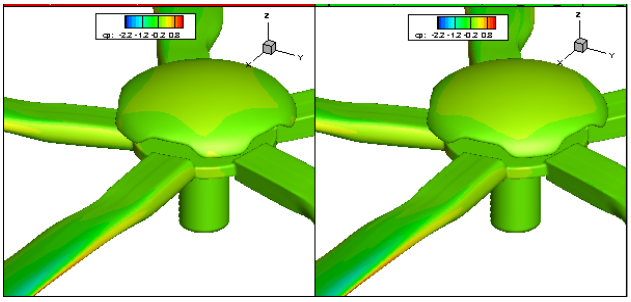

Figure 16. View of the pressure coefficient contour plot over the rotating main rotor hub: comparison of OpenFOAM® (on the right) and ANSYS Fluent® (on the left) results.

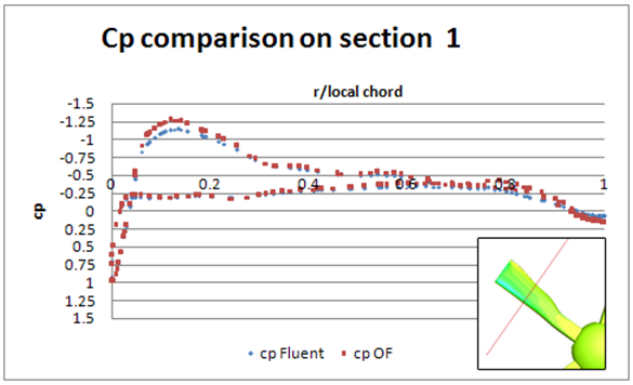

Figure 17. Cp distribution over a blade stub section: comparison of OpenFOAM® and ANSYS Fluent® results.

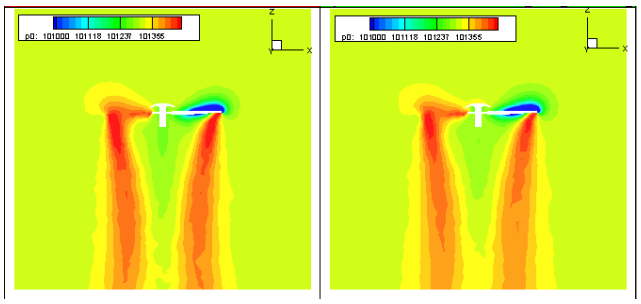

Figure 18. Contours of total pressure over the fluid domain longitudinal midsection: comparison of OpenFOAM® (on the right) and ANSYS Fluent® (on the left) results.

ROTATING HUB IN HOVERING CONDITION

In this second hub test case, the simulations concern the hovering conditions at ISA Sea Level and at an angular velocity equal to 31 rad/s will be discussed.

OpenFOAM® Setup

A simulation was carried out using the newly developed steady-state rhoMRFSimpleFoam solver. As far as the setup of the boundary conditions change from the forward flight hub simulation because the top and bottom box surfaces are now "inlet" and outlet" for hovering configuration and the inlet initial velocity was set to 0 value. The solution strategy was the same of the rotating beanie setup, with a Kinetic Energy value $k=3.41 m^2/s^2$ and a Specific Dissipation Rate value $\omega=4.22 s^{-1}$.

The rotating cylinder surrounding the hub (called "fluid-mrf") was specified to belong to the MRF portion of the domain, hence it was defined within the MRFZones file as a rotating region, with origin (located in (0;0;0)). Other

tests show that this incremental step method is not always necessary.

ANSYS Fluent® Setup
A steady pressure-based solver type with absolute velocity formulation was used for the simulations within ANSYS Fluent®. The same successive steps of angular velocity used in the OpenFOAM® simulation were implemented before achieving the nominal value of rotational speed, in order for the calculation to be more stable. The convergence criterion was established when the RMS residuals were less than 10^{-4} and the other setups were the same of rotating beanie test.

RESULTS.
First of all, the contours of pressure coefficient over the beanie coming from OpenFOAM® and ANSYS Fluent® simulations are compared (one comparison in Figure 16).

Moreover, some sections of the blade stubs were created with the aim of comparing in an accurate way 2D sectional static pressure coefficient distributions calculated using both CFD codes: an excerpt of those comparisons is reported in Figure 17.

As apparent, correlation of OpenFOAM® results with ANSYS Fluent® is very satisfactory, both over the beanie upper surface and the blade stubs. Some minor discrepancies are evidenced over the beanie upper surface, where OpenFOAM® predicts a slightly higher mean value of the static pressure.Concerning the blade stubs' sections, an excellent correlation is found between the two codes over all the considered sections. OpenFOAM® and ANSYS Fluent® predictions of static pressure coefficient are almost coincident all along the blade sections, apart from the suction peak over the airfoil suction side, which is slightly more pronounced in the OpenFOAM® calculation than that predicted by ANSYS Fluent®, especially as far as the inboard sections are concerned.
In Figure 18, both ANSYS Fluent® and OpenFOAM® contour plots of the total pressure are provided in the longitudinal midsection of the fluid domain, with the aim of visualizing the hub wake and quantifying the amount of local dissipative phenomena downstream of the hub. As can be observed, predictions of total pressure losses coming from the two CFD codes are in very satisfactory agreement. Specifically, correlation of the wake shape and intensity (vortex intensity) is very good, with the only difference that the wake predicted by ANSYS Fluent® is slightly more intense in the downstream region next to the domain outlet. Moreover, the streamtube contraction is in good agreement in the two plots, hence suggesting that the generated thrust value predicted by the two codes is very similar, as will be confirmed by the force comparison. In addition, the values of the hub thrust and torque coming from both ANSYS Fluent® and OpenFOAM® are compared were computed. Concerning the thrust (Table 7), an excellent agreement is shown between the two codes, with a percentage deviation between the two codes of around 0.8%. Even correlation on torque is good, a global difference between the two codes of around 7% was registered.

The pressure contribution to torque is predominant according to both OpenFOAM® and ANSYS Fluent®, and the former tends to slightly underestimate it (-3.4%) with respect to the ANSYS Fluent® value, while a larger disagreement is shown on the viscous contribution.

		ANSYS Fluent®	**OpenFOAM®**	**Δ%**
Thrust [N]	**Total**	**1263.3**	**1273.7**	**0.8%**
	pressure	1274	1281.6	0.6%
	viscous	-10.7	-7.9	25.9%
Torque [Nm]	**Total**	**752.4**	**697.7**	**7.3%**
	pressure	647.5	625.1	3.4%
	viscous	104.9	72.6	30.8%

Table 7. Aerodynamic force coefficients of the hovering main rotor hub: comparison of OpenFOAM® and ANSYS Fluent® results.

ROTATING HUB IN FORWARD FLIGHT CONDITIONS

In this third hub test case, the simulations concern the rotating forward flight configuration: specifically, a forward flight speed equal to 120 kts was simulated at ISA Sea Level with an angular velocity equal to 31 rad/s (like rotating beanie test). The same computational mesh used for steady forward flight and hovering simulations (Figure 12) was employed here. Once again it is worth underlying that the dimensions of the virtual wind tunnel are insufficient to avoid blockage effects and the mesh itself is rather coarse. Actually, this caused the simulations not to converge in a proper way, as will be discussed in the following, and a new mesh with different wind tunnel dimension is already under test. However, the emphasis here is on the numerical model feasibility, while a detailed analysis of the simulations' accuracy goes beyond the scope of this work.

OpenFOAM® Setup
The rotating forward flight hub analysis was carried out using the newly developed steady-state rhoMRFSimpleFoam solver. The k-ω SST turbulence model was selected for simulation of viscous effects.As far as the setup of the boundary conditions and solution strategy were the same of the rotating beanie setup in the same analysis condition discussed above, with a Kinetic Energy value $k=3.41 m^2/s^2$ and a Specific Dissipation Rate value $\omega=4.22 s^{-1}$.

ANSYS Fluent® Setup
A steady pressure-based solver type with absolute velocity formulation was used for the non-rotating beanie steady simulations within ANSYS Fluent®. The rotational speed of the MRF zones was set to 31 rad/s counter-clockwise from above the hub. Total temperature, Gauge Total Pressure and Backflow Total Temperature were carried out from initial condition. The convergence criterion was established when the RMS residuals were less than 10^{-4} and the other setups were the same of beanie test.

RESULTS.
Some numerical instabilities occurred using both the CFD codes. Actually, the fluid domain dimensions seemed too small in order for the calculation to converge in a proper way

In fact, in the OpenFOAM® calculation the boundary conditions assigned over the inlet could not be maintained because of the rotating hub being too close to the inlet surface; the contours of pressure coefficient over the beanie coming from OpenFOAM® and ANSYS Fluent® simulations are compared in Figure 19 where, as apparent, correlation of OpenFOAM® results withANSYS Fluent® is good over the beanie, while some major disagreements

are evidenced over the blade stubs. As already mentioned, none of the simulations converged in a proper way; hence the results are not reliable (Figure 20). For these reasons, the computed values of the global aerodynamic coefficients of the rotating hub using the two codes are not reported here, since the comparison could be misleading.

.

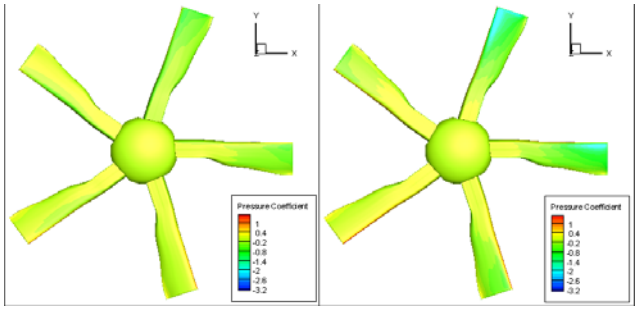

Figure 19. Top view of the pressure coefficient contour plot over the main rotor hub: comparison of OpenFOAM® (on the right) and ANSYS Fluent® (on the left) results.

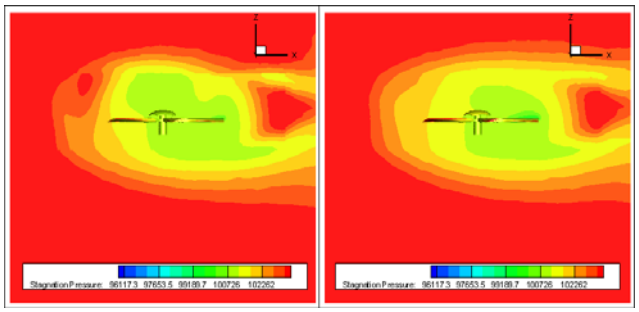

Figure 20. Contours of total pressure of the rotating hub over the fluid domain longitudinal midsection: comparison of OpenFOAM® (on the right) and ANSYS Fluent® (on the left) results.

ACKNOWLEDGMENTS

The authors would like to thank Antonio Saporiti and Carlo Cassinelli from AgustaWestland for their great help and support in the development of the present work. Special thanks to Carlo Cassinelli for his advices in the implementation of the solver rhoMRFSimpleFoam.

REFERENCES

[1] E. Benini, “Contribution to design optimization of tiltrotor components for drag reduction”, JTI-CS-2010-1-GRC-02-004.

[2] E. Gasparella. “Evaluation of an open source computing environment for CFD simulation of helicopter components”, MSc Thesis, University of Padova, 2010.

[3] G. Romanelli and E.Serioli,“A "free" approach to the modern Computational Aeroelasticity”,Politecnico di Milano, 2008.

[4] G. Romanelli, E. Serioli and P. Mantegazza,“A new accurate compressible inviscid solver for aerodynamic applications”, 3rd OpenFOAM® Workshop by Dipartimento di Energetica, Politecnico di Milano, Milan, Italy. July 9-11, 2008.

[5] “OpenFOAM 1.7.1 Documentation”, OpenCFD Ltd., 2010.

[6] “Ansys Fluent 12.0 Documentation”, Ansys. Inc., 2009.

[7] Menter, F. R., "Two-Equation Eddy-Viscosity Turbulence Models for Engineering Applications," AIAA Journal, Vol. 32, No. 8, August 1994, pp. 1598-1605.

[8] S. Petropoulou, “Industrial optimization solutions based on OpenFOAM® technology”, V European Conference on Computational Fluid Dynamics, 2010.

[9] G. Katsaros, F. Campos, “CFD Automatic Optimization using OpenFOAM® in Grid Environments”, National Technical University of Athens.

[10] D. R. Schleicher, J. D. Phillips, K. B. Karbajal, “Design Optimization of High-Speed Proprotor Aircraft”, NASA Technical Memorandum 103988, April 1993

[11] Cicalè, M. (2005). ERICA: The EUROPEAN TILTROTOR, Europe/US International Aviation Safety Conference, Cologne, PowerPoint Presentation.